Total electron loss, charge transfer, and ionization in proton-hydrogen collisions at 10–100 keV

A. Kołakowska and M. S. Pindzola
Department of Physics, Auburn University, Auburn, Alabama 36849

D. R. Schultz
Physics Division, Oak Ridge National Laboratory, Oak Ridge, Tennessee 37831
(Received 16 November 1998)

A three-dimensional lattice solution of the time-dependent Schrödinger equation for low quantum states ($n \leqslant 3$) is combined with classical trajectory Monte Carlo results for high quantum states ($n \geqslant 4$) to predict total electron loss and total charge-transfer cross sections for proton collisions with atomic hydrogen at intermediate energies. The total charge-transfer cross sections range from 5% above to 10% below the furnace target measurements of McClure [Phys. Rev. **148**, 47 (1966)], while the total electron-loss cross sections range from 5% to 15% above the pulsed crossed-beams measurements of Shah, Elliot, and Gilbody [J. Phys. B **20**, 3501 (1987)]. The calculation of ionization as a difference between electron loss and charge transfer leads to theoretical ionization cross sections that are 10% to 35% larger than the crossed-beams measurements of Shah and Gilbody [J. Phys. B **14**, 2361 (1981)] and Shah, Elliott, and Gilbody [J. Phys. B **20**, 2481 (1987)]. [S1050-2947(99)08805-8]

PACS number(s): 34.50.Fa

I. INTRODUCTION

Proton-hydrogen collisions continue to serve as a benchmark for the development of new theoretical methods. The direct solution of the time-dependent Schrödinger equation (TDSE) on a numerical lattice [1–4] has had for many years the potential for yielding accurate inelastic cross sections over a wide energy range. Recently, substantial advances in computer technology have for the first time permitted the implementation of the lattice TDSE method on large three-dimensional grids for the calculation of antiproton and proton collisions with hydrogen [5–7]. Besides yielding accurate cross sections of importance to astrophysical and laboratory plasma research, the lattice TDSE method gives a complete description of the electron dynamics within the quantum-mechanical collision domain found at short interaction lengths.

In recent work [7] we applied the lattice TDSE method to study excitation and charge transfer in proton collisions at energies of 10 to 100 keV with the hydrogen target in its ground state. We used two alternative numerical methods: a low-order finite differences method with a ''staggered leap-frog'' propagator and a high-order Fourier collocation method with a split-operator propagator. It was demonstrated that the cross sections for excitation to the $2s$, $2p$, $3s$, $3p$, and $3d$ subshells of the target and cross sections for capture to the $1s$, $2s$, $2p$, $3s$, $3p$, and $3d$ subshells of the projectile are in good agreement with many recent theoretical and experimental results. The purpose of this paper is to report total cross sections for electron loss, charge transfer, and ionization based on further lattice TDSE calculations for low n shells combined with classical trajectory Monte Carlo (CTMC) calculations for high n shells. In Sec. II we give a brief outline of the computational methods, cross section results are presented in Sec. III, and a brief summary is given in Sec. IV. Atomic units are used throughout unless otherwise noted.

II. THEORY

We consider the time-dependent Schrödinger equation for a bare ion (Z_p) projectile colliding on a straight-line trajectory with a hydrogenic atom (Z_t) target:

$$i\frac{\partial \Psi(\vec{r},t)}{\partial t} = \left(-\frac{1}{2}\nabla^2 - \frac{Z_t}{r} - \frac{Z_p}{R(t)} \right) \Psi(\vec{r},t), \tag{1}$$

where $\vec{r}$ is the electron position vector with respect to the target, and $R(t)$ is the distance between the projectile and the target that is located at the origin of Cartesian coordinates. For example,

$$R(t) = \sqrt{(x-b)^2 + [y-(y_0+vt)]^2 + z^2}, \tag{2}$$

where y_0 and the impact parameter b locate the initial position of the projectile, and v is the projectile velocity. Equation (1) is solved numerically in a rectangular box with the boundary condition $\psi = 0$ at the walls for $t > 0$; and the initial condition $\psi = \psi_{1s}$ in the interior at $t = 0$. Standard numerical techniques are used to avoid spurious wave reflections at the rectangular grid boundaries [7].

Physical observables are obtained by projecting the total wave function following the collision onto the stationary states of the target. The probability of excitation or capture to a $\psi_{n\ell m}$ state is

$$P_{n\ell m}(v,b) = \left| \int d^3r \, \psi^*_{n\ell m}(\vec{r}) \Psi(\vec{r}, t = t_{\max}) \right|^2, \tag{3}$$

where $t_{\max}$ is the propagation time. The cross section for excitation or capture to the $n\ell m$ state is

$$\sigma_{n\ell m}(v) = 2\pi \int_0^\infty db \, b P_{n\ell m}(v,b). \tag{4}$$

Excitation cross sections are computed in the rest frame of the hydrogen atom target, while capture cross sections are computed in the rest frame of the proton projectile.

The total cross section for electron loss from the target can be obtained from the probabilities of excitation by using the relation

$$\sigma_{\rm loss}=2\pi\int_0^\infty db\, b\left(1-\sum_{\rm all\ states}P^{\rm exc}_{n\ell m}(v,b)\right), \tag{5}$$

while the total cross section for charge transfer from the target can be obtained from the probabilities of capture by using the relation

$$\sigma_{\rm trans}=2\pi\int_0^\infty db\, b\left(\sum_{\rm all\ states}P^{\rm cap}_{n\ell m}(v,b)\right), \tag{6}$$

where the summation extends over all bound electron states of the target. In principle, at a given impact energy, the total ionization cross section can be extracted as the difference between the total cross section for electron loss and the total cross section for charge transfer

$$\sigma_{\rm ion}=\sigma_{\rm loss}-\sigma_{\rm trans}. \tag{7}$$

On a finite size lattice the direct solution of the time-dependent Schrodinger equation leads only to a relatively small number of excitation and capture probabilities. To obtain the total electron loss and the total charge transfer, which requires summing the contributions from an infinite number of excited states, the lattice results must be combined with high n-subshell cross sections available using other techniques. In the CTMC method the time evolution of the three-body system is obtained by a classical solution of Hamilton's equations of motion. The initial conditions (i.e., the electron's position and momentum) are chosen randomly from a quantum-mechanical probability distribution. The classical solution is repeated for a large number of projectile trajectories ($\sim 10^6$) to determine cross sections within a statistical accuracy. Good agreement between the CTMC results and experiment can be interpreted as evidence that at high n and intermediate collision energies the three body dynamics are well described by those given by classical trajectories developing from an electronic orbital ensemble chosen to mimic the quantum initial state [8,9].

III. RESULTS

The lattice method and the lattice parameters used in performing the calculations presented in this work are the same as those used before [7]. The low-order finite differences method with a ''staggered-leapfrog'' propagator was applied with a uniform mesh spacing $\delta h=0.2$ in each direction of the cubic box $L=[-30;+30]^3$, and the grid did not include the point (0,0,0). This size of lattice can only support ''spectroscopic'' hydrogenic orbitals for $n=1$, 2, and 3. The Fourier collocation method calculations were performed with spacing $\delta h=0.385$ in a box $L=[-26;+26]^3$, on a grid that included zero. The finite differences calculations were carried out at 10, 25, 40, 60, and 100 keV, while the Fourier collocation calculations were carried out at 40 and 60 keV, corresponding to the peak of the ionization cross section.

TABLE I. Cross sections for the charge transfer to the n shell of the projectile as a function of the proton impact energy in the collision $p+H(1s)$. The units are 10^{-16} cm^2.

E	Finite differences				Total CTMC		
(keV)	$n=1$	$n=2$	$n=3$	Total $n\leqslant 3$	$4\leqslant n\leqslant 20$	$4\leqslant n$	Total
10	7.894	0.534	0.097	8.520	0.024	0.025	8.545
25	2.960	0.563	0.163	3.687	0.095	0.098	3.785
40	1.134	0.282	0.091	1.503	0.101	0.104	1.607
60	0.377	0.096	0.033	0.505	0.052	0.053	0.559
100	0.065	0.015	0.005	0.086	0.008	0.008	0.094

Summaries of the finite difference lattice results for capture to the n-shell of the projectile and for excitation of the n-shell of the target are displayed in Tables I and II, respectively.

The total cross sections for electron loss and charge transfer are calculated by summing up the contributions from all n-shells up to infinity. For this purpose, the lattice results are combined with CTMC results for $n\geqslant 4$. Figure 1 shows a typical CTMC n-level distribution where the computed cross sections fluctuate around a statistical mean that falls off as $1/n^3$. This high-n behavior is also characteristic of the recommended cross section data for excitation compiled by Janev and Smith [10]. The $1/n^3$ scaling relationship can be used to sum up the residual contributions from all n shells above a fixed $n_{\rm max}$ using the $\zeta(3)$ Riemann zeta function. Overall, the CTMC contributions for $n\geqslant 4$ to the total electron loss and charge transfer cross sections are less than 10%, while the contributions above $n_{\rm max}=20$ are extrapolated to be less than 0.3%. The results are summarized in Tables I and II.

In Table III we compare total cross sections obtained with the finite differences method to those obtained with the Fourier collocation method at 40 and 60 keV incident proton energy, corresponding to the peak of the ionization cross section for hydrogen. The Fourier collocation results for electron loss are only 3% lower than the finite differences results, while for charge transfer the Fourier collocation results are roughly 10% higher than the finite difference results. The larger numerical differences found for the total charge transfer is due in part to the added complexity of propagating the atomic probability density across the lattice. The fact that the Fourier collocation results for ionization at 40 keV are almost 15% lower than the finite differences re-

TABLE II. Cross sections for the n-shell excitation of the target and for electron loss as a function of the proton impact energy in the collision $p+H(1s)$. The units are 10^{-16} cm^2.

E	Finite differences			Total CTMC		Loss	
(keV)	$n=2$	$n=3$	Total $n\leqslant 3$	$4\leqslant n\leqslant 20$	$4\leqslant n$	$n=1$	Total
10	0.272	0.072	0.344	0.030	0.031	9.240	8.864
25	0.655	0.154	0.809	0.063	0.064	5.919	5.045
40	0.923	0.210	1.133	0.090	0.092	4.694	3.468
60	1.011	0.213	1.223	0.110	0.113	3.767	2.430
100	0.961	0.182	1.143	0.109	0.112	2.779	1.524

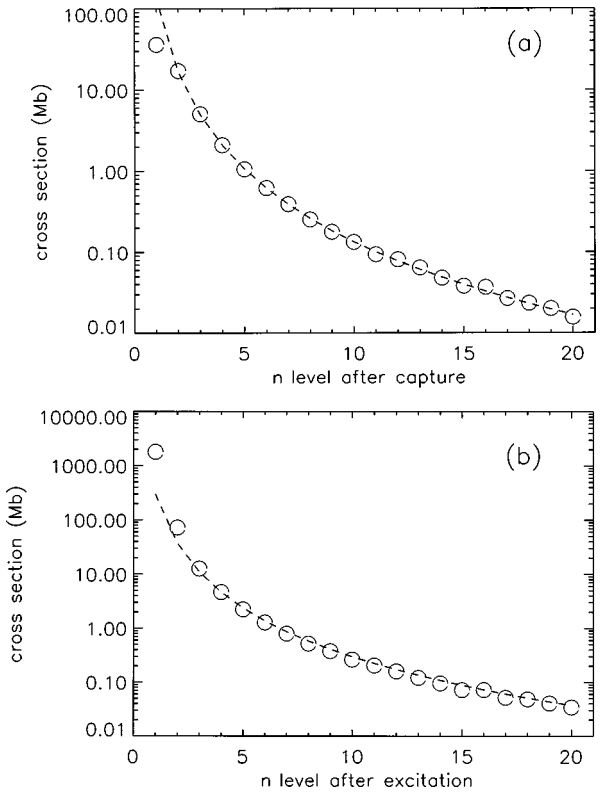

FIG. 1. CTMC cross section n level distributions in the collision $p+H(1s)$ at 60 keV: (a) capture, (b) excitation. The high-n results present statistical (Monte Carlo) fluctuations about a $1/n^3$ behavior (dashed curve).

sults is due in large measure to the relative difference amplification caused by the subtraction of a larger charge transfer cross section from a smaller electron loss cross section.

The finite differences and Fourier collocation calculations for the total charge-transfer cross section are compared with the furnace target measurements of McClure [11] in Fig. 2. The finite differences results are slightly higher than the experimental measurements at low energies and then fall below experiment at the higher energies by at most 10%. The Fourier collocation results are 1% to 5% above the measurements at 40 and 60 keV. If the difference between the two calculations is a reflection of numerical uncertainty, then theory and experiment agree to within their respective error bars for the total charge transfer cross section.

The finite differences and Fourier collocation calculations for the total electron loss cross section are compared with the pulsed crossed-beams measurements of Shah *et al.* [12] in Fig. 3. Both lattice calculational results are 5% to 15% above

TABLE III. The results of blending the CTMC cross sections with finite differences and Fourier collocation methods for the total charge transfer, the total electron loss, and the total ionization. The units are 10^{-16} cm^2.

E	Finite differences			Fourier collocation		
(keV)	Capture	Loss	Ionization	Capture	Loss	Ionization
40	1.607	3.468	1.861	1.804	3.388	1.584
60	0.559	2.430	1.871	0.613	2.347	1.734

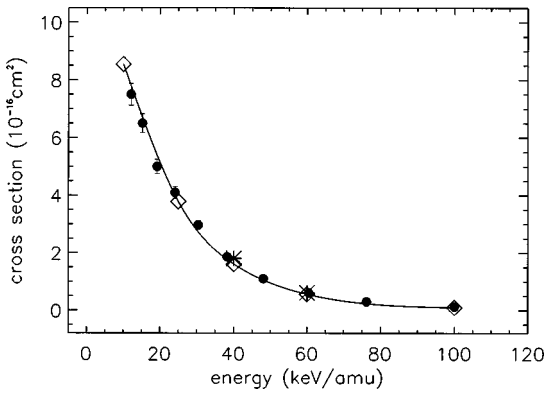

FIG. 2. Total charge-transfer cross section as a function of proton impact energy. The solid curve presents the cubic spline interpolation of values computed with the finite differences method (diamonds). The asterisks present the results of Fourier collocation method. A comparison is made with experimental results of McClure [11] (filled circles).

the measurements over the entire energy range. Thus, theory and experiment are in slight disagreement for the total electron loss cross section.

The total ionization cross section is extracted by taking the difference between the total electron loss and the total charge transfer cross sections. The finite differences and Fourier collocation calculations for the total ionization cross section are compared to the crossed-beams measurements of Shah and Gilbody [13] and Shah *et al.* [14] in Fig. 4. At the peak of the ionization cross section the finite differences results are 30% to 35% above the experimental measurements, while the Fourier collocation results are 10% to 25% above the measurements. Although the predicted shape of the ionization cross section as a function of proton energy agrees well with experiment, the slight disagreement between theory and experiment for the electron loss cross section has been amplified by the use of Eq. (7) to obtain the total ionization cross section.

The main contribution to the total cross sections for electron loss and charge transfer comes from the lattice TDSE results for the $n\leqslant 3$ shells. In order to check whether the

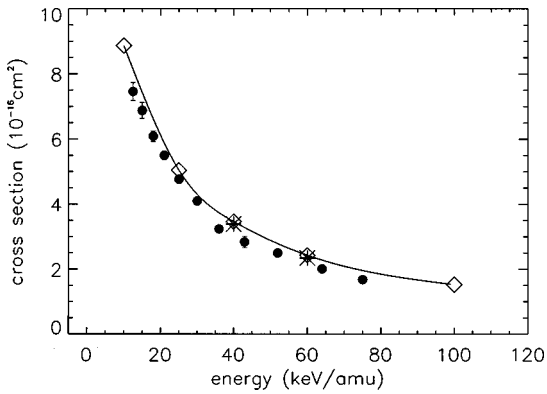

FIG. 3. Total electron-loss cross section as a function of proton impact energy. The solid curve presents the cubic spline interpolation of values computed with the finite differences method (diamonds). The asterisks present the results of the Fourier collocation method. A comparison is made with the experimental results of Shah *et al.* [12] (filled circles).

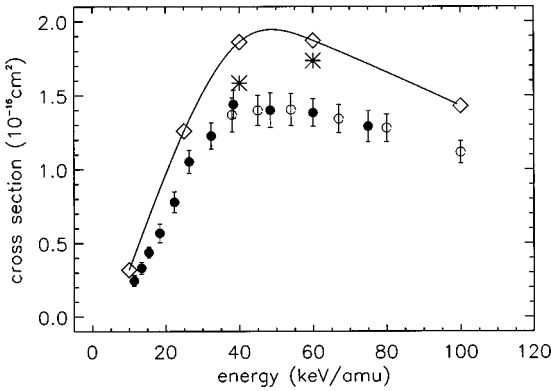

FIG. 4. Total ionization cross section as a function of proton impact energy. The solid curve presents cubic spline interpolation of values computed with the finite differences method (diamonds). The asterisks present the results of the Fourier collocation method. A comparison is made with the experimental results of Shah and Gilbody [13] (open circles) and Shah *et al.* [14] (filled circles).

differences found in the two numerical methods are reasonable, we tested the sensitivity of the finite difference results by varying selected lattice parameters. We reduced the mesh spacing from $\delta h = 0.20$ to $\delta h = 0.15$ keeping the box size the same and then repeated the electron loss and charge transfer calculations at 60 keV. The excitation cross sections changed by 2% to 4%, while the capture cross sections varied from 2% to 6%. Calculations were also carried out at 100 keV using different combinations of mesh spacing and box size with at most a 2% effect on contributions from the $n \leqslant 2$ shells. We repeated the finite difference calculations at 60 keV on a grid that included zero and found almost no change in the excitation and capture cross sections.

A smaller contribution to the total cross sections for electron loss and charge transfer comes from the CTMC results for the $n \geqslant 4$ shells. At the peak of the ionization cross section, the CTMC calculations for the $n \geqslant 4$ shells only contribute between 3% to 5% of the total electron loss cross section and 6% to 9% of the total charge transfer cross section. Thus, even substantial changes in the CTMC results for the $n \geqslant 4$ shells translates into fairly small changes in the total cross sections.

IV. SUMMARY

Total cross sections for electron loss and charge transfer in proton collisions with hydrogen in the 10–100 keV intermediate energy range are calculated using a lattice TDSE method for the $n \leqslant 3$ shells combined with a CTMC method for the $n \geqslant 4$ shells. The theoretical cross sections for total charge transfer are in reasonable agreement with the furnace target measurements of McClure [11], while the calculated cross sections for total electron loss are uniformly 5% to 15% above the pulsed crossed-beams measurements of Shah *et al.* [12]. The theoretical peak cross sections for total ionization are between 10% and 35% above the crossed-beams measurements of Shah and Gilbody [13] and Shah *et al.* [14]. The large relative discrepancy between theory and experiment can be mainly attributed to the indirect approach of extracting ionization cross sections in a way that amplifies the uncertainties in the determination of the electron-loss and charge-transfer cross sections. Further work is needed to develop a more direct method for the extraction of ionization probabilities and cross sections. In the meantime the steady advance in computer technology promises to continually decrease the numerical uncertainty in atomic cross section methods based on the direct solution of the time-dependent Schrödinger equation.

ACKNOWLEDGMENTS

We would like to thank F. Robicheaux and K. Bartschat for many useful discussions, and M. B. Shah for providing us with the electron-loss experimental results in numerical form. In this work, A. Kolakowska and M. S. Pindzola were supported in part by a National Science Foundation grant to Auburn University, while D. R. Schultz was supported by the U.S. DOE Office of Basic Energy Sciences and Office of Fusion Energy Sciences at Oak Ridge National Laboratory, managed by Lockheed-Martin Energy Research Corporation under Contract No. DE-AC05-96OR22464. The computational work was carried out at the National Energy Research Supercomputer Center in Berkeley, CA.

[1] V. Maruhn-Rezwani, N. Grün, and W. Scheid, Phys. Rev. Lett. **43**, 512 (1979).
[2] C. Bottcher, Phys. Rev. Lett. **48**, 85 (1982).
[3] K. C. Kulander, K. R. Sandhya Devi, and S. E. Koonin, Phys. Rev. A **25**, 2968 (1982).
[4] J. D. Garcia, Nucl. Instrum. Methods Phys. Res. A **240**, 552 (1985).
[5] D. R. Schultz, P. S. Krstic, C. O. Reinhold, and J. C. Wells, Phys. Rev. Lett. **76**, 2882 (1996).
[6] J. C. Wells, D. R. Schultz, P. Gavras, and M. S. Pindzola, Phys. Rev. A **54**, 593 (1996).
[7] A. Kolakowska, M. S. Pindzola, F. Robicheaux, D. R. Schultz, and J. C. Wells, Phys. Rev. A **58**, 2872 (1998).
[8] C. O. Reinhold, R. E. Olson, and W. Fritsch, Phys. Rev. A **41**, 4837 (1990).
[9] D. R. Schultz, R. E. Olson, C. O. Reinhold, M. W. Gealy, G. W. Kerby III, Y.-Y. Hsu, and M. E. Rudd, J. Phys. B **24**, L599 (1991).
[10] R. K. Janev and J. J. Smith, Nucl. Fusion Suppl. **4**, 1 (1993).
[11] G. W. McClure, Phys. Rev. A **148**, 47 (1966).
[12] M. B. Shah, D. S. Elliott, and H. B. Gilbody, J. Phys. B **20**, 3501 (1987).
[13] M. B. Shah and H. B. Gilbody, J. Phys. B **14**, 2361 (1981).
[14] M. B. Shah, D. S. Elliott, and H. B. Gilbody, J. Phys. B **20**, 2481 (1987).